UDC 550.837.211: 477.41:451.14

Svetlana KOVÁČIKOVÁ[1], Igor LOGVINOV[2'], Viktor TARASOV[2]

[1] Institute of Geophysics, Acad. Sci. Czech Republic, Bocni II/1401, Praha 4-14131, Czech Republic, e-mail: svk@ig.cas.cz, [1]https://orcid.org/ 0000-0003-2600-175X
[2, 3] Subbotin Institute of Geophysics. Nation. Acad. Sci. of Ukraine, 32, Palladin av., Kyiv, 03142, Ukraine,
e-mail: anna_log@ukr.net, [2]https://orcid.org/ 0000-0002-9584-0314, [3] https://orcid.org/ 0000-0001-9906-9259

https://doi.org/10.23939/jgd2022.02.099

AREA-WIDE 2D AND QUASI-3D GEOELECTRIC MODELS OF THE EARTH'S CRUST AND UPPER MANTLE AS A POSSIBLE EVIDENCE OF RECENT TECTONIC ACTIVITY IN THE WESTERN PART OF THE UKRAINIAN SHIELD

The purpose of the presented work was to model the electrical conductivity distribution in the northwestern part of the Ukrainian shield and to study the relationship of geoelectric anomalies with natural mineral deposits and with signs of possible tectonic activation of long-lived fault systems on the Shield. The methodology was based on long-period magnetotelluric and magnetovariational measurements in the period range of 3–16 to 2500–3600 s. The dense network of measurement sites made it possible to explore the geoelectric structure of the Ukrainian Shield segment limited by the coordinates 26°–30°E and 48°-51,7°N. 2D and quasi-3D inversion of the obtained magnetotelluric and geomagnetic responses resulted in the creation of overview models of electrical resistivity/conductivity for the territory of investigation. As a result, geoelectrically anomalous structures were identified at different depths. The local character of the conductors and their position indicate their connection with recently activated fault zones, their junctions and with metallogeny. The Precambrian age of crystalline rocks of the investigated area refers mainly to the electronic-type graphite-sulphite origin of increased conductivity, however the depth of conductive features, their vertical extent and their link to rejuvenated fault systems may indicate the genetic connection of various minerals and their subsequent precipitation with deep fluid migration. Originality. The obtained results aimed at clarifying the deep structure and correlating the geoelectric features of the earth's crust and upper mantle with fault systems and deposits of various natural mineral sources. In addition, they alone can serve as further evidence of possible tectonic activation processes in the studied area. Practical significance. The presented results can bring social benefits by identifying areas of mineral endowment, and in the field of geodynamics they can contribute to the assessment of natural hazard in mapping the course of tectonically active fault systems.

Key words: Earth's crust and upper mantle; East European Platform; Ukrainian Shield; electrical conductivity; mineralization.

Introduction

Precambrian terranes are considered tectonically inactive since their formation, with a thick inert lithosphere and low heat flow. Episodically, however, their reactivation may occur, manifested by lithosphere weakening, heat flux anomalies, hot springs, melt enrichment, with corresponding density anomalies, fault rejuvenation, and unexpected intraplate seismic activity [Foley, 2008]. Such phenomena are documented on various ancient terranes [Chatto-padhyay et al., 2020]. Recent and current intraplate tectonic activity may be associated with the impact of post-glacial rebound in areas that have experienced continental glacial history [Wu et al., 1999], with stress controlled by interactions of distant plate boundaries and its migration along existing ancient fault systems [Parfeevets and Sankov, 2018], with mantle convection (Wang et al., 2015) and activation of ancient continental failed rift systems [Lough et al., 2018].

The Ukrainian Shield (USh) represents an exposed basement of the Precambrian East European Platform (EEP) (Fig. 1). From the northeast, the USh is separated from the crystalline Voronezh Massif (VM) by the Dnepr-Donets Basin (DDB), filled in the Paleozoic by thick (up to 16 km in the southeast) sediments. The northern continuation of the DDB is formed by the Pripyat' depression (PD). Then the USh is surrounded by the Caledonian Volyn-Podolian Plate (VPP) in the west, the Paleogene-to-Neogene Black Sea Lowland (BSL) in the south and the Hercynian Donets Ridge (DR) in the southeast (Fig. 1a). Thick sedimentary complexes northwest of the USh are known as the Volyn-Polesie belt (VPb) (Fig. 1b).

The Shield is intersected by deep fault zones and sutures (Fig. 1a, Fig. 2), which divide it into megablocks. The oldest faults on the USh originating in the Neoarchean have a predominantly northwest-southeastern orientation [Ryabenko,1970; Sollogub et al., 1980]. The north-south oriented shear zones were formed at the first stage of the Paleoproterozoic (PR_1-I) [Bogdanova et al., 2008]. Then the NW-SE faults were reactivated at the later Paleoproterozoic (PR_1-II). The system of latitudinal fault zones of the USh was created at the end of the Paleoproterozoic – the beginning of the Mesoproterozoic (PR_1-PR_2) [Gintov and Pashkevich, 2010]. Between 1.8–1.47 Ga, the USh was intruded by plutonic structures, such as the Korosten pluton (Kpl) or Korsun-Novomirgorod pluton (*KNpl*) (Fig. 1a, b) [Bogdanova et al., 2006].

Although we consider the USh a stable structure, its revitalization repeatedly occurred in the Hercynian and Alpine periods, accompanied by magmatism, hydrothermal processes, ore mineralization and hydrocarbons, appearance of deep xenoparticles in sediments, uplift and erosion of blocks and crustal thinning [Gordienko et al., 2005; 2012]. Signs of current activity can still be observed. They include anomalous heat flow, gravity anomalies in the mantle, negative seismic velocity anomalies in the crust, earthquakes (especially on the southwestern periphery of the shield), and Helium isotope anomalies. Their manifestation is mostly concentrated at the northwestern USh boundary with the DDB and in the basin itself, at the southwestern USh boundary with the VPP and in the central and the eastern part of the Shield (Fig. 2a) [Gordienko et al., 2020].

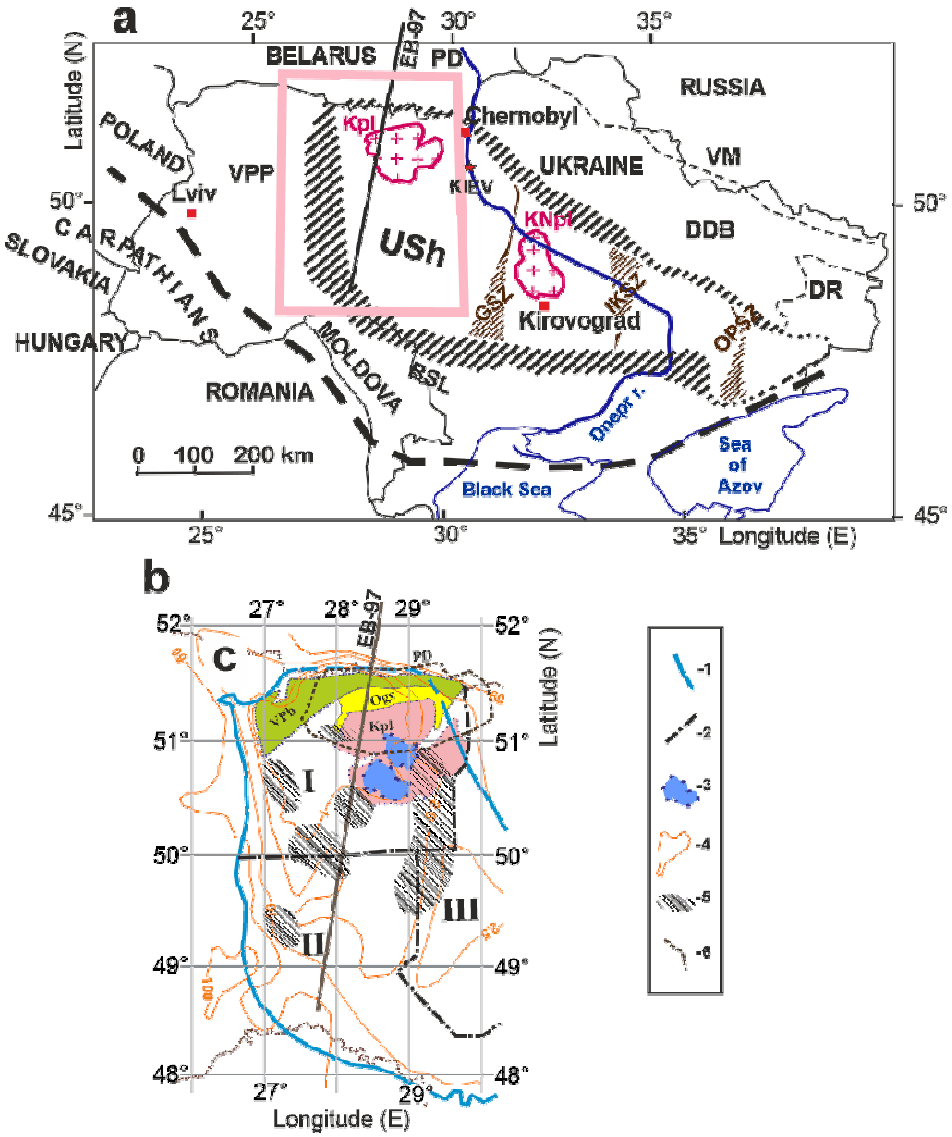

Fig. 1. a – location of the studied area (rectangle):
USh – Ukrainian Shield with the slopes (black dashed areas), BSL – Black Sea Lowland, DDB – Dnieper-Donets Basin, DR – Donets Ridge, PD – Pripyat' Depression, VM – Voronezh Massif, VPP – Volyn-Podolian Plate; EB-97 – International seismic profile EUROBRIDGE'97; plutons: Kpl – Korosten, KNpl – Korsun-Novomirgorod; thick dashed line – EEP southern margin; brown dashed areas – suture zones: GSZ-Golovanevsk, IKSZ-Ingulets-Krivyi Rih, OPSZ-Orekhov-Pavlograd.
b – studied area – detail of the rectangle in the subfigure (a):
1 – zero contour of the Riphean deposits [Baysarovich et al., 2002], tectonic elements [Gursky et al., 2007]: 2 – megablock boundaries (roman numerals): I – Volyn, II – Dnister-Bug, III – Ros-Tikich; VPb – Volyn-Polesie belt, Ogs – Ovruch graben-syncline, Kpl – as in subfigure (a); 3 – deposits of gabbro-anorthosite formation; 4 – Integrated conductivity (conductance) of sediments (S_{sed}) in Siemens; 5 – south-western graphite-bearing areas (SWGR); 6 – delimitation of the North-Ukrainian oil and gas province (NUOGP) [Map…, 2004]; EB-97 – as in subfigure (a).

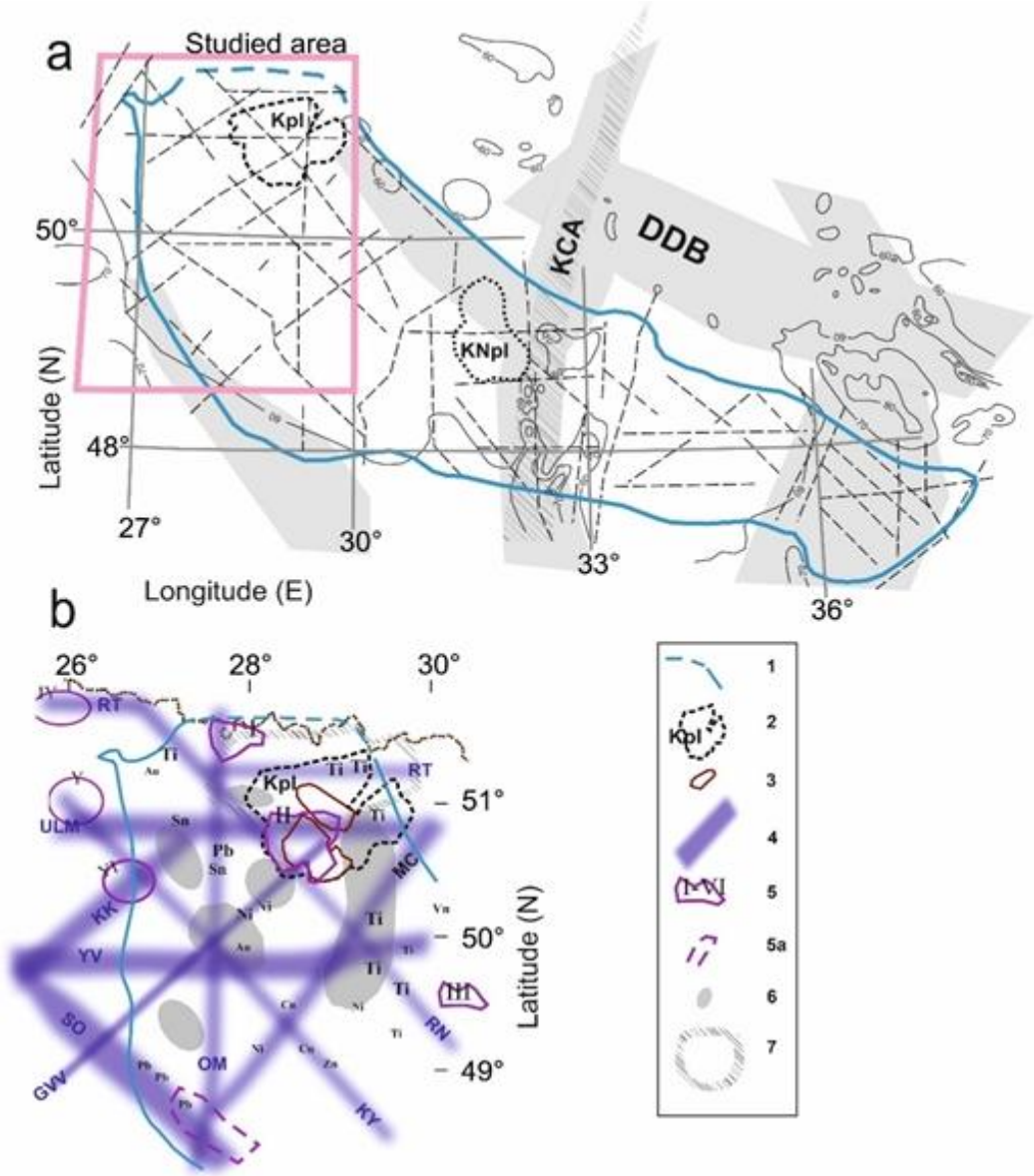

Fig 2. a) – fault system network of the USh (thin dashed lines); zones of recent activation (grey areas) [Gordienko et al., 2020] and increased heat flow areas (contours in mW/m^2) [Gordienko et al., 2002]; Kpl and KNpl – Korosten and Korsun-Novomirgorod plutons (as in Fig. 1a); KCA (dashed belt) – Kirovograd conductivity anomaly [Gordienko et al., 2005]; b) – fault systems and metallogeny of the study area [Baysarovich et al., 2002]; 1 – USh contour; 2 – Korosten pluton contour, 3 – gabbro-anorthosite formation (core of the Korosten pluton); 4 – faults active in last 3 million years [Verkhovtsev, 2006]: OM – Olevsk-Murava; RT-Ratnov-Terniany, ULM – Ust' Lug-Malyn, YV – Yavoriv-Volchansk, KK – Khust-Khorets, GVV – Gusyatin-Volodarsk-Volyn, MC – Murava-Chernobyl, RN – Rakitnov-Novoarkhangelsk, KY – Kamen'Kashirski-Yalta, SO – Sokal'-Odessa; occurrences of minerals with electron–type conductivity: 5 – ore nodes [Baysarovich et al., 2002; Prikhodko and Prikhodko, 2005], 5a – manifestation of lead-zinc mineralization; 6 – graphite-bearing areas of the North-West Graphite Region NWGR [Yatsenko, 1998]; 7 – NUOGP delineation.

Among other signs of tectonic activity, the central part of the USh is also manifested by the prominent Kirovograd electrical conductivity anomaly (Fig. 2a), traced from the Black sea in the south and traversing the DDB [Gordienko et al., 2005; 2006]. The study of the electrical conductivity/resistivity distribution in the Earth provides further insight into the material composition and geological and tectonic structure of the Earth's interior [Karato and Wang, 2013] and can serve as another indicator of the presence of conductive mineralized fluids in fault systems, carbonaceous material or partial melt associated with activation processes.

The area of present study covers the western part of the USh and is characterized by the occurrence of deposits of minerals with electron-type conductivity

(graphite, polymetals, noble metals) [Shcherbak, Bobrov, 2006] with electrical conductivity significantly different from the host crystalline rocks. Fig. 2b presents data on metallogeny of the region and fault systems active in recent 3 million years [Verkhovtsev, 2006]. Areas where more than three known mineral deposits occur are combined into ore knots. Node I contains deposits of Cu, Pb, Ti, Li, Br, Sn; node II – Ti, Vn, Au; node III – Ti; nodes IY and YI – Cu; node Y – Cu, Pb, Zn. Abbreviations of elements correspond to individual deposits (increased letters correspond to the proximity of 2 deposits). The territory also hosts the North-West Graphite Region (NWGR) [Yatsenko, 1998] as well as one of the promising areas for the occurrence of hydrocarbons, the North Ukrainian Oil and Gas Province (NUOGP) [Starostenko, 2004] (Fig. 1b; Fig. 2b).

Geological and geophysical studies (including magnetotelluric, MT) by the Ukrainian State Geological Exploration Institute (UkrGGRI) and the Northern State Regional Geological Survey "Pivnichgeologia" (SGRGP) in the NUOGP territory have revealed the most promising areas from the point of view of possible accumulation of hydrocarbons - the Ovruch graben-syncline (Ogs) and the VPb adjacent to the PD, where Precambrian basement submerges beneath a thick strata of the Paleozoic sediments (Fig. 1b). Within these areas, seismic surveys revealed zones of increased fracturing, dipping towards the depression. Based on the results of a formal interpretation of MT soundings, a conductive layer in the upper part of the crystalline basement was revealed. It refers to the rock decompression zone [Tregubenko et al., 2009]. Later, 2D inversion of MT data along the seismic international profile EUROBRIDGE'97 [Ilchenko 2002; Thybo et al., 2003] intersecting NUOGP made it possible to identify electrically anomalous structures. They correlated with the distribution of seismic velocities V_p and related to the zone of flank faults at the southern margin of the PD and within the Ogs [Astapenko and Logvinov, 2014]. Listric faults identified in seismic geological sections crossing the PD are assumed to act as a path for hydrocarbon migration from the territory of the PD to Ogs [Garetsky and Klushin, 1989].

The Ukrainian territory has been covered by numerous geophysical studies. A dense network of MT data collected over the past 50 years made it possible to reveal electrically conductive structures also on the territory of the USh [Ingerov et al., 1999; Gordienko et al., 2005; Logvinov, 2015]. On the basis of a formal interpretation of MT sounding curves in the northwestern part of the USh. A local electrical conductivity anomaly related to the Kpl was revealed on the basis of a formal interpretation of MT sounding curves in the northwestern part of the USh [Burakhovich et al., 1997]. 2D inversion of MT data for the whole territory of Ukraine east of the longitude 25.4°E collected before 2017 made it possible to reveal a number of low resistivity structures in the earth's crust and upper mantle of the territory under discussion [Logvinov and Tarasov, 2019]. Some of these objects were in good agreement with knots of ore minerals concentration.

In previous works of the authors, the geoelectric parameters of the earth's crust and upper mantle of Ukraine were estimated using 1D and 2D inversions of MT data [Gordienko et al., 2005; 2006; 2012; Logvinov, 2015; Logvinov et al., 2017; Logvinov and Tarasov, 2019]. Based on magnetovariational data (MV, only magnetic components of MT field), the areal distribution of the integrated conductivity (conductance *S*) of the earth's crust of the Carpathians and adjacent part of the EEP was analyzed using quasi-3D inversion [Kováčiková et al., 2019]. As a result, the presence of numerous high conductivity / low resistivity structures (r <100 ohmm) has been confirmed in the earth's crust of the VPP.

This paper presents the results of 2D inverse modeling using TE, TM and TP modes of MT data in the period range of 1–3600 s along a network of 12 latitudinal and 16 longitudinal profiles intersecting the Korosten pluton and the Ogs (see Fig. 3a). The study also considers quasi-3D (thin sheet) inversion of MV data in the period range of 100–900 s, making it possible to estimate the geoelectric parameters of the earth's crust and upper mantle of the western part of the USh limited by coordinates 26°–30° E and 48°–51.7° N (Fig. 1a). Compared to previous studies up to 2017, a denser network and new experimental data allowed us to reduce the bandwidths of the profiles. The aim of the work was to clarify the distribution of electrical resistivity and it is inverse, i. e. Conductivity, and explain the behavior of MT interpretation parameters obtained from MT and MV soundings in the studied territory. The distribution of electrically anomalous features and their correlation with geological data (association with a network of fault systems, metallogeny, graphite and hydrocarbon deposits) leads to considerations about their formation mechanisms and interconnections. This can contribute to tracing active fault systems and knowledge of tectonic processes in ancient areas with awakening tectonic activity currently or in the recent past.

Geology

The western part of the USh is formed by the Volyn, Dnestr-Bug and Ros-Tikich megablocks [Claesson et al., 2014] (Fig. 1c). The Volyn domain is mainly of Paleoproterozoic age (PR_1) and is composed of gneisses and crystalline schists. It is intruded by the Korosten pluton (Kpl) formed during the unstable period of the platform development. The Dniester-Buh (or also Podolian) megablock is composed of prevailing Archaean-Paleoproterozoic (AR-PR_1) granulites, quartzites and biotite gneisses with gneisses, crystalline schists, granites and migmatites in the lower section. The Ros-Tikich megablock on the east is formed mainly by diorites, basalts and Archaean gneisses and crystalline schists in the upper part of the section.

In Fig. 1c and the following figures, the shield boundaries are marked by the zero contour of the Riphean deposits (a Meso- to Neoproterozoic PR_2-PR_3 sequence of the geological timescale 1.65–0.65 Ga old, used in the EEP Proterozoic stratigraphy). This approach is conditioned by the presence of much younger Mz-Kz sediments with a thickness of 50–250 m, irregularly covering supracrystalline, ultra-metamorphic and intrusive rocks, which belong to the Prebaikalian (Preriphean) EEP basement. Proterozoic is the age of the basement rocks in most of the studied area. Archaean rocks occur only in the south and east (Fig. 3a). According to [Baysarovich et al., 2002], this situation reflects the beginning of the formation of the EEP sedimentary cover structures associated with the accumulation of continental dark-colored terrigenous formation (middle- and upper Riphean) of the Polesian series (represented by clay rocks lying at the base, and sequences of sandstones and siltstones above them), filling VPb. Within the Ogs, the bottom of the section of the Ovruch series belongs to the Riphean, while the upper part is composed of pink quartzite-sandstones with thin layers of terrigenous-effusive pyrophyllite schists.

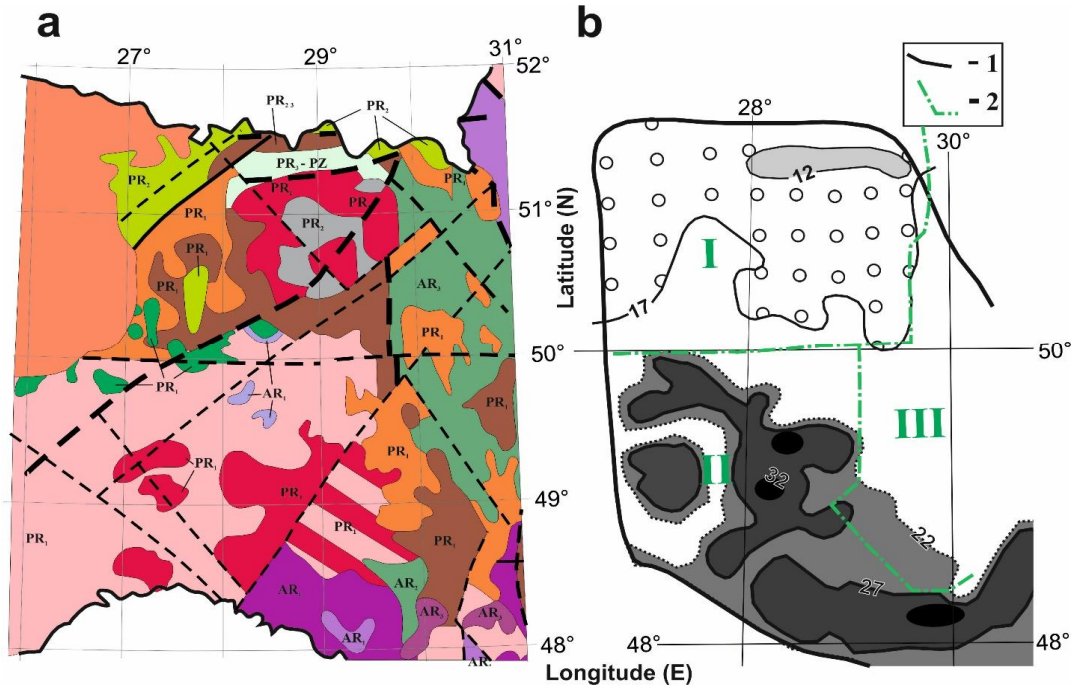

Fig. 3. a – geological section of the Preriphean rocks [Baysarovich et al., 2002]; b – erosional discordance depth (ΔH) for the northwestern part of the Ush, (in km), 1 – the zero contour of the Riphean deposits, 2 – megablock boundaries (roman numerals – see Fig. 1c).

Rocks of various metamorphic facies of the Archean (3.7–2.8 Ga) to early- and middle Proterozoic (2.2–1.9 Ga) are exposed on the USh (mostly amphibolite, more scarcely granulite, epidote-amphibolite, greenschists). Riphean rocks occur in a limited extent only on the western and southwestern edges of the Shield and in the Ogs. Following text refers to the work of [Gordienko et al., 2005]. Preriphean rocks were formed under the pressure and temperature conditions corresponding to the depth interval of 7–37 km. It seems that the erosional truncation (ΔH) in the shield is significant and varies strongly from region to region depending on different amplitudes of uplift. Typical temperature distribution over depth (pressure) for the whole USh crust (that meets the regional metamorphism conditions) was constructed in [Garetsky and Klushin, 1989]. Then the typical depth interval for each facies and subfacies was estimated according to the map of metamorphic facies for the USh [Usenko, 1982]. Fig. 3b presents a fragment of the map of the erosional discordance surface for the USh [Gordienko et al., 2005]. Contour lines are drawn with 5 km step, which corresponds to a triple error in determining ΔH. The Volyn block is characterized by the smallest values of the erosional discordance (less than 17 km), while typical depths for the Dniester-Buh block are more than 22 km.

The research area is characterized by a number of unique geological features. The most impressive is the Middle Proterozoic (1.8–1.75 Ga) Korosten pluton (Kpl in Fig. 1c and Fig. 2 and corresponding PR_1-PR_2 structure in Fig. 3a) in the northwest part of the Shield, which belongs to the Volyn domain, and according to geologists is associated with the most mobile zone, the "hot spot" of the crystalline basement. The core of the pluton is occupied by anorthosite and gabbro formations, surrounded by younger rapakivi-type granites. The width of the contact zone of rapakivi granites with gabro-anorthosite massifs does not exceed 1.2–1.5 km. The

main minerals of the gabro-anorthosite complex are titanium and apatite. In the northern part of the Volyn block, adjacent to the Kpl, Meso-to-Cenozoic (Mz-Kz) effusive sedimentary deposits of the Ogs are embedded on the eroded surface of granites of the Kpl complex (PR_3-*Pz* mainly sub-latitudinal structure in Fig. 2a). In fact, the Ogs is formed by three interconnected depressions – central Ovruch (about 110 km in length and 20 km in width) with latitudinal strike and smaller submeridional Belokorovichi, adjacent to the west, and Vilchani to the east. Deposits of noble and non-ferrous metals were revealed in the depression sediments. One of important factors, which can explain the nature of conductivity anomalies is the content of graphite in crystalline rocks. The NWGR is one of the large graphite regions of the USh. According to [Yatsenko, 1998], Ukraine accounts for about 7.9 million metric tons of graphite reserves. Varying thicknesses and, consequently, electrical apparent resistivities are reflected in the conductance (integrated electrical conductivity) map of the surface sediments S_{sed}, which on the USh does not exceed 10 S, while Riphean deposits are responsible for its 6–10 times increase (Fig. 4b).

Purpose

The purpose of the presented work was to create a quasi-3D geoelectric model of the northwestern USh segment and analyze of the link of electrically conductive structures to fault systems, their junctions and associated mineral deposits and the relationship of geoelectric anomalies with tectonic activity within fault systems on the Shield.

Experimental data and geoelectric research methods

In the presented work, we used MT data in the range of periods from 1–16 s to 2500–3600s, obtained by several Ukrainian and Belarussian prospecting organizations under the direction of V. Tregubenko, A. Ingerov, V. Astapenko [Ingerov et al., 1999; Astapenko, 2012] and employees of the Institute of Geophysics of the National Academy of Sciences of Ukraine (IG NASU) (Fig. 3). A detailed summary of the results is given in [Gordienko et al., 2005, 2012; Kovacikova et al., 2016; Logvinov, 2015; Logvinov et al., 2017, 2020].

2D inversion. First, the experimental data were interpreted using the 2D REBOCC inverse modeling procedure [Siripunvaraporn and Egbert, 2000] along profiles crisscrossing the area. In the modeling procedure, MT sounding curves and vertical magnetic transfer function were used. In previous works [Logvinov 2015; Logvinov and Tarasov, 2018, 2019; Logvinov et al., 2017, 2020] the whole territory of Ukraine was gradually intersected by a dense network of 2D inverse models.

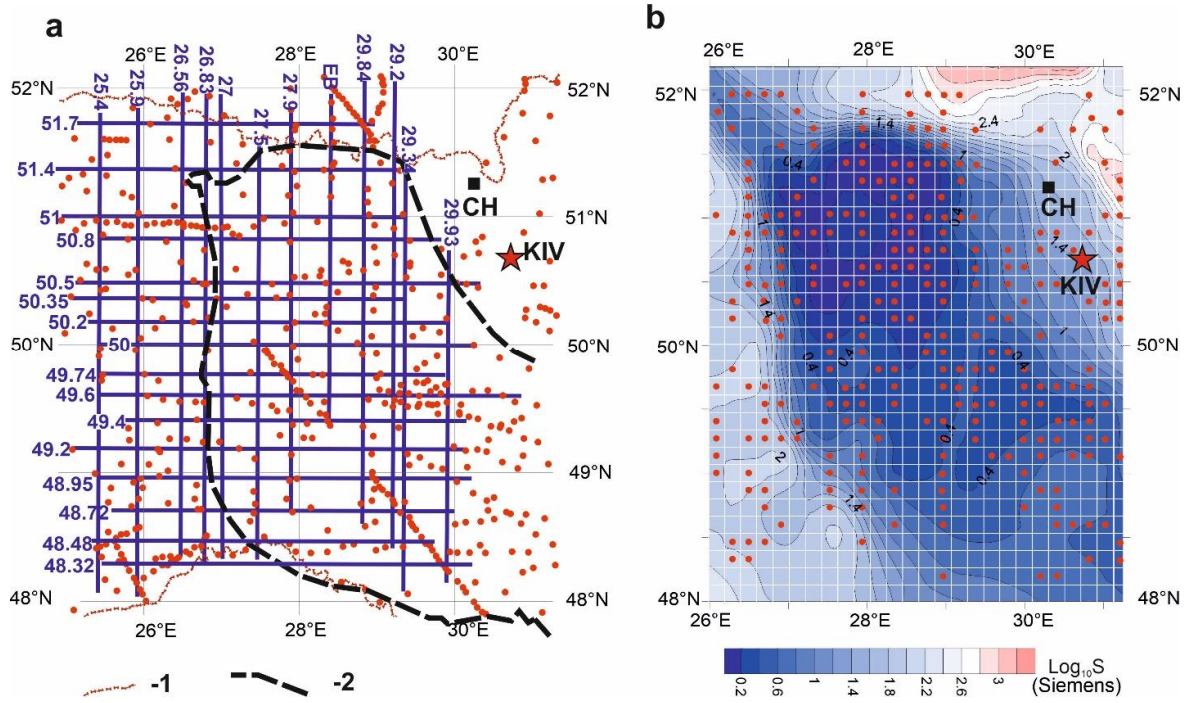

Fig. 4. a – sites of the observed MT field in the USh and contiguous areas (red dots):
KIV – Kyiv geomagnetic observatory (star), CH – area of Chernobyl nuclear power plant accident (black square); 1 – Ukrainian state boundary, 2 – USh boundary;
b – map of the surface sediments S_{sed} for the studied area and MT sites (points) used in Quasi-3D inversion:
network of 15 km×15 km cells (white squares) for the selection of the area for the quasi-3D modeling.

The values of MT probing curves performed by reconnaissance organizations are estimated with an accuracy that usually does not exceed 15 % in amplitude and 3–5° in phase. Since most of the data used in the simulation was obtained by exploration organizations, we assumed errors proportional to the triple error in determining each simulation parameter in the REBOCC procedure: 0.1 for magnetic transfer functions, 10 % for the impedance phase, 30 % for visible resistivity. Previous studies have found the presence of low-impedance structures with different extensions. Because the MT probing curves provided by the reconnaissance organizations were presented only for 0° and 90° azimuths, the interpretation profiles were located in the latitudinal and meridional directions.

The density of 2D data suggested their areal presentation. Details of the method were described in [Tarasov and Logvinov, 2020]. Of course, we are aware of the danger of presenting 3D structures using 2D results. Recently, 3D inverse modeling has been widespread in geoelectric studies (e.g. [Siripunvaraporn et al, 2005; Kelbert et al., 2014]), however, it is a non-linear and non-unique problem with a number of unknown inversion parameters at the input. The areal presentation of 2D data provided a general view of the distribution of geoelectrically anomalous features over a large area and can serve as an intermediate step on the way to completing 3D detailed modeling of individual structures.

The area of construction of the volume geoelectric model included the territory of the northwestern segment of the USh and part of the VPP adjacent to the west (26°–30°E, 48°–51.7°N). Data of 9–11 periods (in the range of 1–3600 s) were used in the procedure. In the interpretation, magnetotelluric data at 445 points from almost 690 points available on the territory of the western part of the USh and the adjacent part of the VPP were used. According to the applied procedure described in detail in [Logvinov, 2015], the choice of MTS sites was conditioned by the availability of impedance phases and TE, TM and TP modes in at least 75 % of the used frequency range.

The horizontal step varied from 3 to 10 km. The step along the vertical axis was 100–500 m for the upper 2 km and 1000–4000 m for the depth interval of 2–50 km. Below, the step varied from 8 to 30 km. The applied MT data frequency range (between 1–16 and 2500–3600 s) and the dimensions of the studied area (the profile lengths 256–421 km) allowed creating a reasonable geoelectric model reaching a depth of 110 km. Compared to previous results (up to 2017, cited above), new experimental geoelectric data were used in this work, including records obtained in 2019 and the exact coordinates of observation points obtained by exploration organizations. When compiling the initial interpretative models, a priori geological and geophysical information on the structure of the region was used. The sedimentary cover thickness in the territory of the Republic of Belarus was calculated according to [Makhnach et al., 2001]. When specifying the starting models, the S_{sed} values for the PD sediments were taken according to [Astapenko, 2012], and for the USh according to [Tregubenko et al., 2009].

MT probing is based on electromagnetic induction in conductive media, so most of the information about the presence of conductive structures is contained in the longitudinal curves of MT probing (TE mode) and vertical magnetic components (TP mode). With this in mind, the simulation began using TE and TP interpretation parameters. The obtained models with the smallest root mean square values (mean squares) values for each mode were used for further modeling with two or more modes.

Quasi 3D inversion using the thin sheet method. In 2D modeling, a significant number of vertical magnetic responses was not incorporated. Some of the points in which magnetic responses were available did not fall on the belts of 2D modeling profiles. The others were not used because the number of points with defined magnetic responses on profiles did not satisfy the requirement of having at least 70 % of TP mode data. The purpose of applying thin-sheet modeling was to: 1) clarify the spatial position of anomalous objects that explained the behavior of the vertical magnetic transfer function in the studied area, 2) compare the results with 2D inversion models. The procedure is based on interpretation of purely magnetic responses of MT field and on the thin-sheet approach, i.e. on the assumption that the Earth's crust and upper mantle layers are thin enough compared with the wave length and penetration depth of the applied MT field periods and can be considered as thin sheets. In quasi-3D modeling, interpretation parameters were single-station vertical magnetic transfer functions, components of real (C_u) and imaginary (C_v) induction vectors indicating the relationship between the three components of the magnetic field in the frequency domain. In this work, induction vectors in the Wiese convention were used. A detailed description of the inversion technique is given in [Kováčiková et al., 2005] and applied to MT studies in Ukraine in [Gordienko et al., 2005; 2006; 2012].

The quasi-3D modeling area was limited by longitudes 26–31.2°E and latitudes 48–52°N. To define the modeling area, the whole western part of the EEP in Ukrainian territory was divided into squares with a side of 15 km and the area with the highest density of points with recorded data (available in 275 cells of a total of 652, which was 42 %) was selected (Fig. 4b). According to the results of 2D modeling (see *Modelling results*), the depth to the top of the conductive structures in the earth's crust varies in the depth interval of 3–30 km and their central parts are located at depths of 11, 16, 20 and 30 km. Considering S_{sed} values for the USh, it can be expected that already at a period of 100 s, the conductive structures located at depths of less than 10–11 km can contribute to the MT field. Therefore,

the calculations were performed for periods of 100, 400 and 900 s. The number of cells surrounding the modeling area was about 25 %. Although according to the S_{sed} map (Fig. 4b) the sub-surface rocks are mostly non-conductive. In order to assess the influence of conductive sediments on the edges of the Shield, a two-sheets inversion was performed with a first surface sheet with fixed conductance and a second sheet with unknown *S*. The parameters of the input 1D model from top to bottom were as follows: the 1st layer 0.5 km thick corresponds to a sheet with a fixed S_{sed} conductance (Fig. 4b;) [Semenov et al., 2008; Logvinov, 2015]; 2nd layer 10.5 km thick with an electrical conductivity of 0.001 S/m; 3 – anomalous thin sheet (inversion result); 4 – 100 km with conductivity 0.00333 S/m, 5 – 100 km with conductivity of 0.01 S/m, 6 – half-space with conductivity 0.001 S/m. The depth of the anomalous sheet of 11 km was selected with respect to the 2D modeling results and analysis of the equivalent current distribution for an equivalent sheet located at different depths [Banks, 1979; Kováčiková et al., 2005]. Deeper, the smooth distribution of current functions becomes unstable. This indicates the transition of the field below the source upper boundary. Selection of the normal conductance at the thin sheet margins showed that the most satisfactory value was 400S.

Modeling results

2D modeling results. Before proceeding to discuss the results of modeling, it is necessary to assess thedegree of agreement between the observed and model data. Fig. 5 shows the RMS value for all profiles. The symbols on the graphs correspond to the root mean square values: total – total discrepancy taking into account the use of all 6 parameters of interpretation; inconsistencies of values: apparent resistivity TE and TM – TE-Rho (TM-Rho) and impedance phase – TE-phase (TM-phase); real and imaginary parts of magnetic responses – TP-Cu (TP-Cv) for all points and all periods. International practice of using the REBOCC inversion procedure shows that a good approximation of experimental data to a two-dimensional model is observed at rms values not exceeding 2–2.2. Among the longitudinal only for profiles 29.2° and 29.93° the value of the root mean square value slightly exceeds the specified interval. Among the latitudinal profiles, the root mean square value exceeds 2.2 for the profiles of 48.32°, 49.4° and 51.7°. The TE-Rho mismatch on all profiles is less than 2.2, while the TE phase exceeds this value for three longitudinal and six latitudinal profiles. The RMS value for the TP mode exceeds the specified value only on the 29.34° profile. The largest number of profiles with rms values exceeding 2.2 values occurs for the TM phase. The above rms indicate a fairly good correspondence between the parameters of the interpretation of the 2D model. Note that a rms value not exceeding 2–2.2 means that the rms value for all points and all periods for each mode is less than the specified value in 75 % of cases.

Fig. 6 shows the model distribution at different depth levels, obtained by jointly using the TE, TP, and TM modes. On all profiles of the models, zones with <120 ohmm can be distinguished. Such r values are much smaller than the generally accepted values for crystalline rocks of the Earth's crust. Their contours practically coincided with areas with r <60 ohmm. Let us call them the low-resistivity objects (LRO). The MT methods do not have not strong resolution with respect to high-resistivity rocks. Therefore, changes in high r values are reflected in sections by areas within the intervals 40–120, 120–3000 and more than 3000 ohmm (called high-resistivity objects HRO).

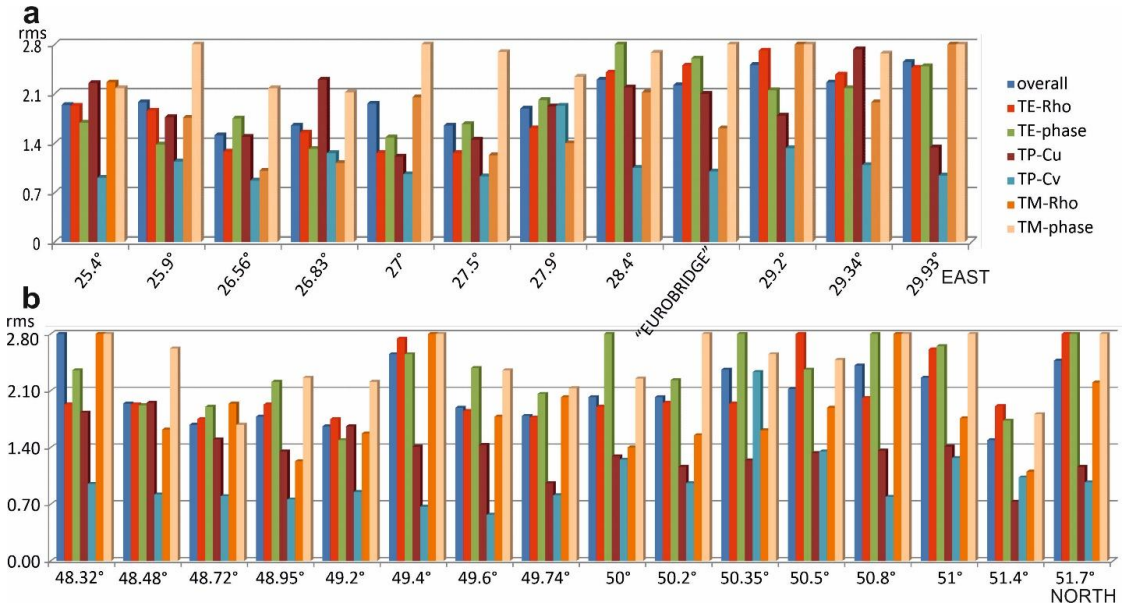

Fig. 5. RMS deviations for longitudinal (a) and latitudinal (b) 2D profiles.

According to the results of laboratory experiments on direct and alternating current, the resistivity of rocks composing the crystalline basement of the Earth's crust and upper mantle to a depth of 100-200 km reaches hundreds of ohmm. In this framework, there are inclusions reducing the resistivity of rocks – sections with increased porosity containing mineralized water, enriched with ore minerals, graphitized rocks, fluids and partially melted rocks.

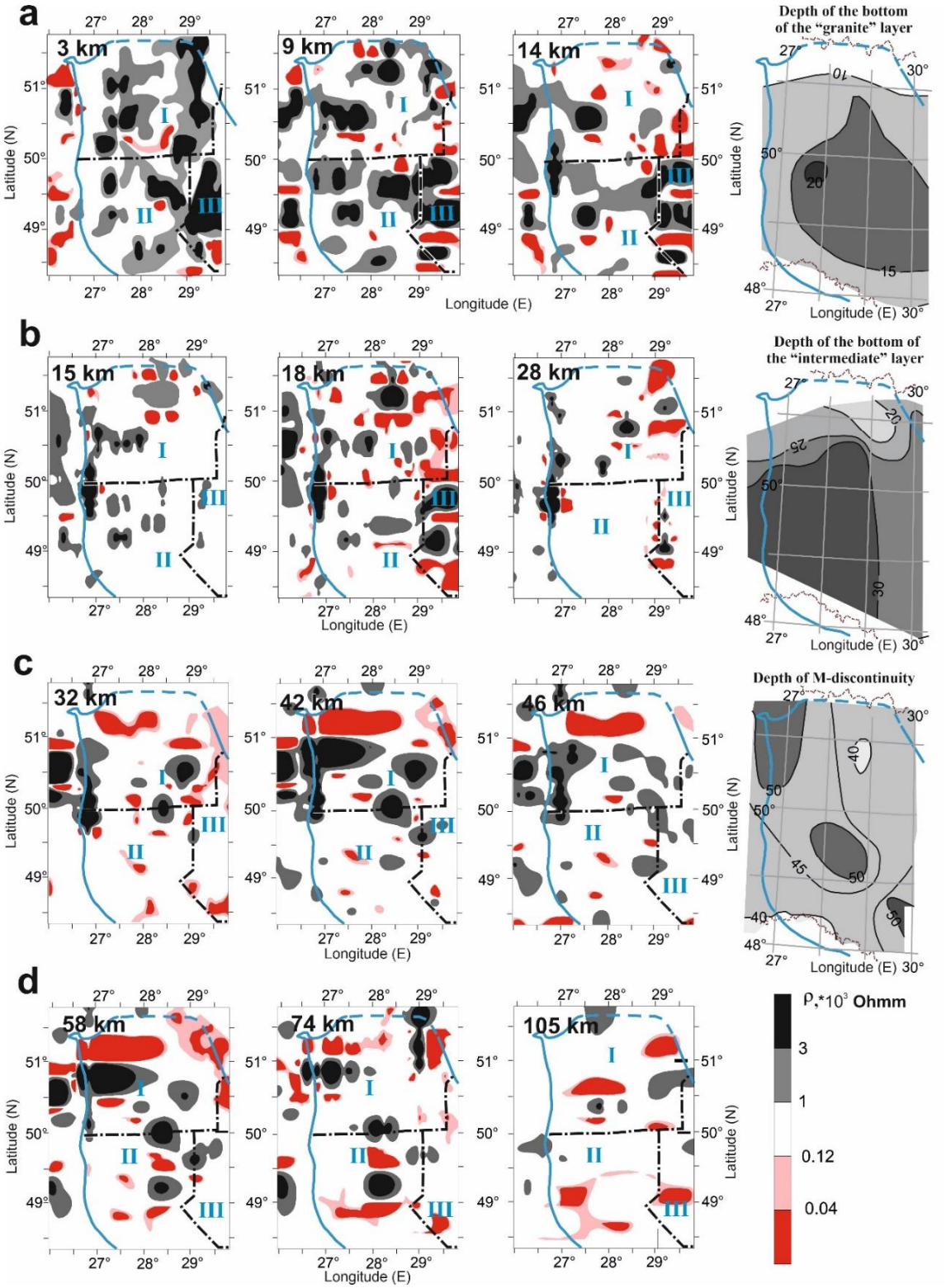

Fig. 6. Resistivity distribution in different layers of the Earth's crust and mantle: a – in depths of the "granite" layer; b – in depths of the "intermediate" layer; c – in depths of the "basaltic" layer; d – in the mantle depth.

Currently, due to the irregular density of observation points, it is difficult to confidently estimate in detail geoelectric characteristics of the anomalous objects. To justify the size of the objects depicted on the slices, the recommendations and guidelines for creating maps set out in cartography textbooks were used ([Salishchev, 1987] and others). Taking into account the density of modeling profiles, the map scale of the available points of MT observations equal to 1:2000000 can be selected. Based on the above and taking into account the existing norms for geophysical maps [Salishchev, 1987], the minimum sizes for objects selected on sections can be more than 100 km^2. The least reliable data were obtained for the southern margin of the USh and east of longitude 29.3°E. In the first of these areas, there is a lack of experimental data (and the available ones are characterized by MT sounding curves in a limited range of periods and the absence of impedance phases and magnetic responses).

The area limited by coordinates 29.3°–31°E and 51.2°–52°N refers to the restricted zone of the Chernobyl nuclear power plant accident (upper right corner on Fig. 6; see Fig. 1a, Fig. 4).

Let us consider the distribution of geoelectric parameters in accordance with the schemes of thicknesses of the Earth's crust layers (on the right of subfigures 6a, b and c) (after [Gordienko et al., 2005]), plotted according to seismic data on regional profiles. Three layers are traditionally considered: "granite" (V_p up to 6.4 km/s), "intermediate" (V_p up to 6.8 km/s) and "basaltic" (down to the Moho boundary, V_p up to 7.2 km/s).

As follows from the distribution of ρ presented in Fig. 5, no continuous conductive layers are observed in any section down to the depth of 105 km. The number and size of local low-resistivity structures varies with depth. In the "granite" layer, the amount of LROs suddenly decreases at the boundary with the intermediate layer. Then, an increase in the number of LROs with depth (down to 18 km) is observed in the intermediate layer. In the "basaltic" layer, the number of LROs does not increase, but several large structures appear. They are most pronounced at mantle depths in the interval of approximately 50–70 km (Fig. 6d). Spatially, the largest number of conductive structures in all depth intervals occur in the Volyn block (I) of the USh, specifically in the lower crust and upper mantle. Some LROs are related to the Ros-Tikich (III) area close to its border with the Dnestr-Bug (II) block. The fewest structures appear on the western border of the USh and in the Dniester-Buh block. The largest portion of the studied area is occupied by high-resistivity rocks. Despite the different lithological composition of rocks exposed on the Prevendian section (the latest stage of the Neoproterozoic up to the beginning of the Cambrian 650–543 Ma), the rock resistivity over most of the territory at all depth levels does not exceed 3000 ohmm. The analysis shows that the area occupied by blocks with the highest resistivity (with ρ >3000 ohmm) significantly decreases with depth. Their greatest manifestation is recorded in the "granite" layer. At the same time, in the western part of the USh between latitudes 49.5°–51°N, HROs are still present throughout the whole studied range of depth

Quasi-3D modelling results. Subfigures a, b and c of Fig. 7 show models of the conductance for the three periods 100, 400 and 900s respectively, together with the fit of recorded and model induction vectors. Fig. 6d presents a comparison of the resistivity distribution (2D inverse models) at a depth of 10 km and the conductance distribution in a thin sheet (quasi-3D inversion) obtained as a result of joint inversion for all three periods. In most cases, the LRO's and the high conductivity features are located in the same areas. Only in the central part of the studied area (between longitudes 28° and 29°E and latitudes 50.5° and 51°N), the conductive structures according to the thin-sheet model are not accompanied by LRO's resulting from the 2D inversion. The magnetic components of the MT field are assumed to be less susceptible to distortion of the industrial origin. Therefore, it is now possible to estimate the geoelectric parameters of the section between longitudes 30 and 31°E. The discrepancy in the spatial size of the anomalous structures in both models can be explained taking into account the differences in cell sizes in both modeling approaches.

The geomagnetic depth sounding technique is poorly sensitive to high resistivity features, as EM induction does not occur in such structures and, therefore, magnetovariational anomalies of the MT field do not appear there. Nevertheless, a comparison of the results of the two methods shows (Fig. 7d) that objects of increased conductivity *S* are located outside blocks of high-resistivity rocks identified by 2D modeling. Since the quasi-3D inversion made it possible to obtain the model of wider area, at all three investigated periods, east of the longitude 30°E, we can see a prominent conductive effect of the Golovanevsk suture zone, which is nevertheless outside our study area (see Fig. 1a), delimiting the Dniester-Buh and Ros-Tikich domains from the east. Anomalous feature of the suture was studied in various papers (e.g. [Antsiferov et al.,2011; Shirkov et al., 2017]) and its nature might be associated with the tectonomagmatic activation and fluid transport in the crust and mantle.

Discussion

The nature of electrical conductivity anomalies is associated with an increased content of electron-type or ionic conductors in rocks, which in turn are associated with tectonic processes in the Earth. Electron-type conductors are represented by minerals containing polymetals and graphite, ionic conductors include partially melted rocks, mineralized waters and fluids (increased concentration of which can occur in fault zones).

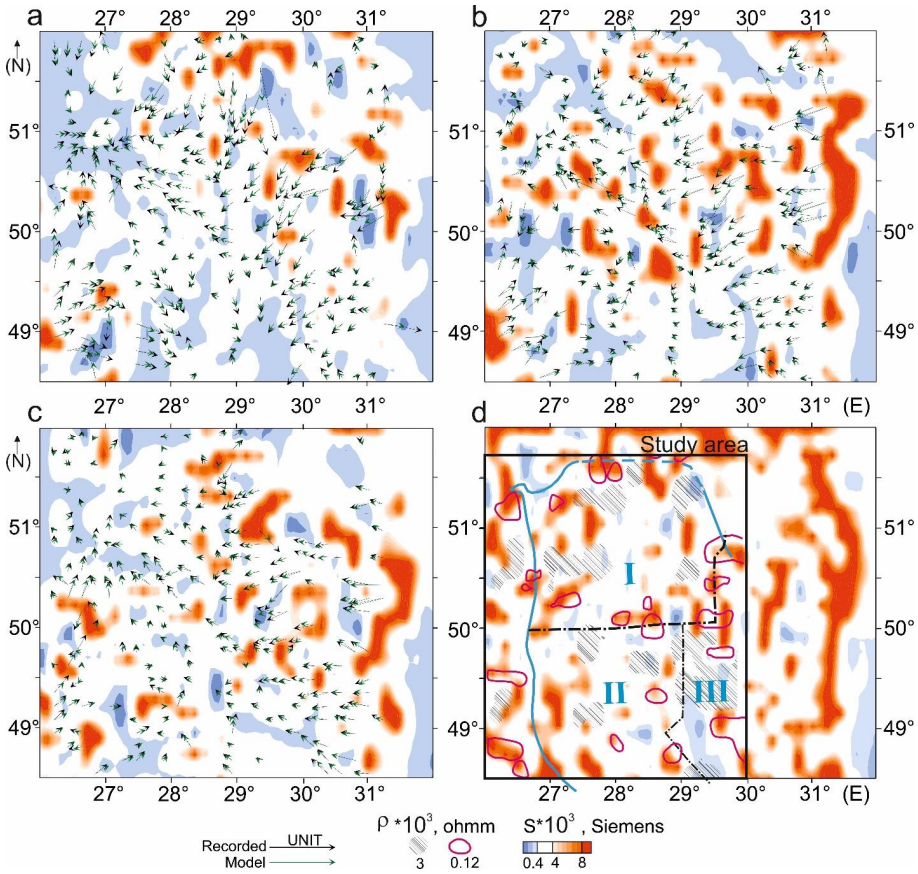

Fig. 7. Conductance distribution for periods of 100 (a), 400 (b) and 900 s (c) respectively in the thin sheet at a depth of 11 km (quasi-3D inverse model) and fit of the recorded (black) and model (green) real induction vectors; d) – joint conductance distribution for periods 100+400+900s and its comparison with distribution of the high- and low-resistivity structures at the corresponding depth obtained from the 2D modeling.

In regions with active tectonics, crustal and upper mantle conductors are often associated with fluid transport or partial melt (for all others, [Jodicke et al., 2006]). On the other hand, in ancient stable shields due to mylonitization in fossil shear zones and low porosity of highly metamorphic rocks, fluid loss occurs during deformation, and the existence of low-resistivity structures in the earth's crust and upper mantle of crystalline terranes is more likely associated with the sulphite-graphite content in metasediments and metavolcanites of high metamorphic stages and in basic and ultrabasic rocks (e.g. [Korja et al., 2002; Bouzid et al., 2015; Yin et al., 2014; Kaplun 2018; Sarafian et al., 2018; Malleswari et al., 2019]).

Based on the analysis of physical properties, an increase in the basicity of rocks with depth is recorded, according to the rock composition model of the earth's crust of the considered area [Gordienko et al., 2005]. Laboratory studies were conducted on various mineral complexes of the Archaean and Proterozoic age of the USh rocks. They showed that the USh rock resistivity reached tens of thousands of ohm [Shepel, 2003]. It should be noted that laboratory measurements are carried out on rock samples taken from complexes exposed on the earth's surface, i.e. possible changes in mineral and aggregate composition of rocks that occur at great depths are not taken into account. The recorded geoelectric data indicate that in the earth's crust an expansion of areas of rocks with $r < 3000$ ohmm (Fig. 6) with depth is observed, which (according to laboratory measurements) is difficult to explain by the effect of temperature increase with depth. To explain this fact, it is necessary to assume the enrichment of deep seated rocks with conductive inclusions that reduce the conductivity of large volumes of rocks. The local character of the conductive objects and the location of metallogenic zones (see Fig. 2b) may indicate their connection with fault zones. In further analysis, only regional features of the geoelectric parameters were used. The aim of the analysis was to show the possible connection of the identified conductive structures with regional tectonic elements and metallogeny. The observed conductivity anomalies reflect the current state of the deep Earth's structure, therefore, it is logical to compare the conductivity structure with faults active in the last 3 million years (Fig. 2b, Fig. 8).

According to geological estimates [Gursky et al., 2003], the thicknesses of individual suites and series of Proterozoic rocks varies between several hundred

meters and 8 km in ancient sedimentary structures. The depth of development of mineral deposits does not exceed 1 km. Consistent with these arguments and the resolution of geoelectric modeling (the size of LROs cannot correspond to the mineral deposits), the comparison was carried out using horizontal geoelectric sections at depths where the central portions of the LROs are located (Fig. 7). Unlike the southern boundary of the USh [Logvinov and Tarasov, 2018], there is no clear connection between the low resistivity structures and the western boundary of the USh (following the zero contour of the Preriphean basement).

An elongated high resistivity zone can be distinguished along the USh boundary between latitudes 49.5° and 50.5° N below a depth of 14km. The northern and northwestern margin of the USh (falling into the NUOGP oil and gas province, see Fig. 1c; Fig. 2b) is marked by conductivity anomalies not only at shallow levels corresponding to the sedimentary fill of the Ogs, VPb and PD (where the sedimentary strata thickness reaches 6 km) but even deeper, in the thin sheet conductivity model (11 km depth) and in 2D models at various depths, probably associated with hydrocarbon migration along the PD flank faults.

Although the picture of the distribution of geoelectric parameters in Fig. 7 looks rather complex, it is possible to observe the concentration of anomalous conductivity/resistivity structures along individual faults and at their intersections (with which mineral deposits with electron-type conductivity are often associated) at different depths.

Let us proceed to the analysis of the Olevsk-Murava (OM) longitudinal fault zone. Along the fault and at its intersection with other faults, there are a number of deposits concentrated in node I, lead-zinc and other mineralization and graphite-bearing areas of the NWGR. In the upper part of the 'granite' layer, down to a depth of 7–9 km between 49° and 51° N latitude, several high-resistivity structures intersect the OM.

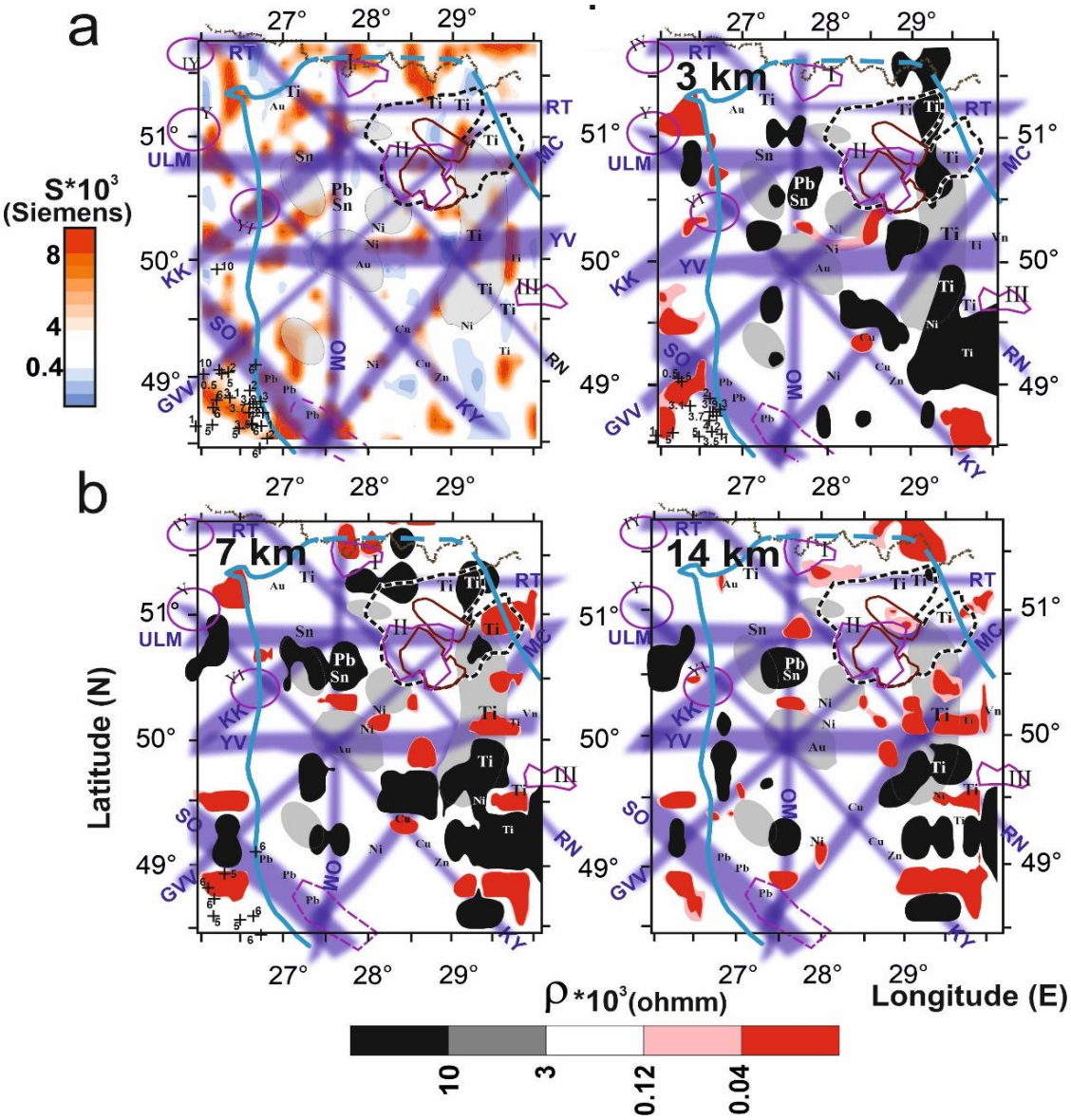

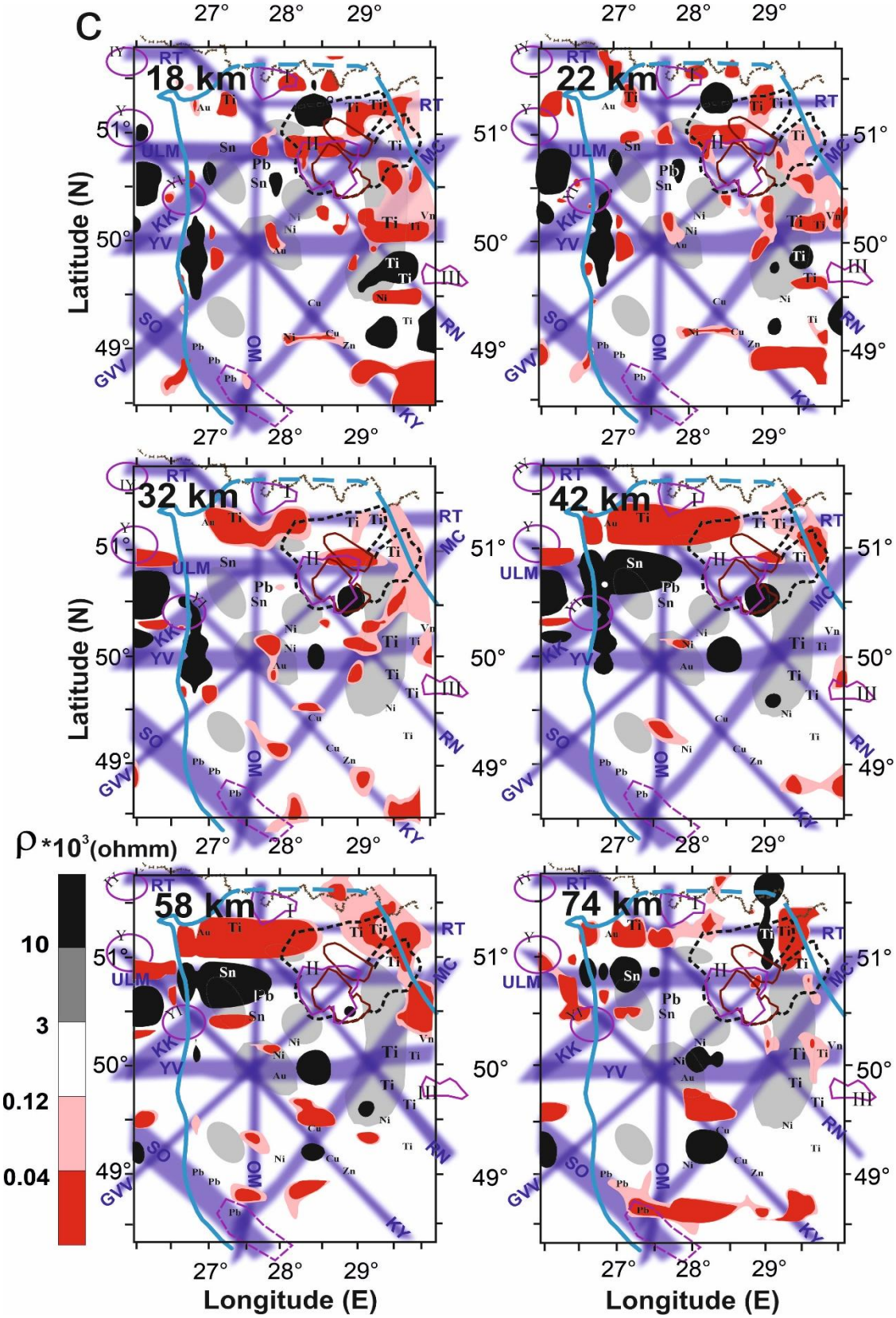

Fig. 8. Correlation of the geoelectric parameters with metallogeny and fault tectonics:
(a), (b) in the granite layer; (c) in the lower crust and upper mantle horizons.
a – the quasi-3D joint inverse model for periods 100–400–900s for the thin sheet at the depth of 10 km.
b, c – models calculated using the 2D inversion. Geological and tectonic information – see Fig. 2b.
Black crosses on subfigures (a) and (b) – seismic events with their focal depths
in corresponding depth intervals (Seismological bulletins of Ukraine for the years 2002–2016).

Deeper than 10 km, down to the mantle depths, resistive blocks practically disappear and conductive structures appear. One of them is in quite good agreement with one of the graphite-bearing areas and ore mineralization (intersection of OM with a latitudinal and two diagonal faults at approximately 50° N latitude). Another conductive structure appears along the fault at approximately 51° N latitude (again linked to the fault junction and one of the graphite-bearing areas) in the thin-sheet model (Fig. 8a) at a depth of 11 km, although not seen in the resistivity models (2D modeling results, Fig. 8b, c).

There are three latitudinal fault zones in the study area. Above a depth of 9 km, HROs appear along the Ratnov-Terniany (RT) zone and the northern side of the Kpl. A single object also appears in the depth interval of 18–24 km. Local structures, which appear in the interval of 11–24 km, form one latitudinal low-resistivity structure along the whole fault zone at depths of 30–74 km. At a depth of more than 7 km and reaching 32 km, local LROs appear along the Ust Lug – Malyn (ULM) fault located southward. One of them seems to be related to the core structure of the Kpl, some of them extend into the node II and the graphite-bearing area of the NWGR. In the depth interval of 16–30 km, the objects form a latitudinal chain. In the depth interval of 35–90 km, HROs form a latitudinal zone extending from the western slope of the USh to the intersection with the OM fault. Local objects connected with metallogeny can be distinguished in different segments of the Yavoriv-Volchansk (YV) zone, often at the intersections of several faults. Some conductive structures seem to be arranged at the periphery of the graphite-bearing areas (above the depth of 14 km, Fig. 8a, b). Deeper than 30 km, a high-resistivity block appears.

Among the three northwest-southeast striking faults, the Rakitnov – Novoarkhangelsk (RN) is most fully characterized by geoelectric parameters. Along the RN fault zone mainly titanium deposits occur. The largest high-resistivity block hosting one of the groups of Ti deposits is located in the southeastern part. The number and spatial extent of objects decreases with depth and at a depth of more than 25 km they disappear. Local conductors, which can be linked to the fault, are distinguished in different parts of the zone southeast of the latitude 51° N down to the depth of 35 km. A number of polymetallic mineralization deposits (mainly copper) are associated with the Kamen' Kashirski – Yalta (KY) fault. Several local high-resistivity blocks, which do not correlate with the location of the polymetallic deposits, appear along the strike of the fault. At crustal depths, high-resistivity blocks often alternate with LROs, some of which correlate with metal deposits. In the lower crust and upper mantle, the LROs are concentrated at the intersections of several faults.

Although no noticeable geoelectric anomalies coincide directly with the Sokal – Odessa (SO) fault itself, a conductive structure appears along the SO fault, but further south (in some sources Podolian fault, e.g. [Map…, 1988]), corresponding to the USh edge dipping to the southwest and its boundary with the VPP (Fig. 8a). The area coincides with one of the maximum vertical uplifts on the USh in the last 3 Ma (reaching 100 m) and correlates with the zone of increased heat flow reaching 60 mW/m^2 (see Fig. 2a), which, according to [Gordienko et al., 2005, 2012], does not exclude partial melting in the depth interval between 35 km and the Moho boundary and fluids retained in between layers.

According to the Seismological bulletins of Ukraine for the years 2002–2016, moderate seismicity in the studied area occurs on the western border of the USh and the VPP (Fig. 8a, b). Events with earthquake duration magnitudes M_d<3 occur above a depth of 10 km (with two events at a depth of 10 km), they are located again between the GVV and SO faults (except for one event near the KK) and seem to be arranged along the SO fault zone, although south from the surface fault course itself (the fault is dipping to the southwest). They appear to be linked to conductors, but surround the most conductive areas. Such behavior associated with fluids migration in faults zones has been described, for example, in [Unsworth and Bedrosian, 2004] and reported in tectonically active regions (e.g. [Srebrov et al., 2018; Kováčiková et al., 2016, 2019]. The aseismicity of the rest of the region may be due to the fact that the level exceeding the critical elastic stress (for rock strength) has not yet been reached.

A significant number of deposits of minerals with an electron-type conductivity is confined to the intersection of the southwest striking faults with other fault zones. Let's begin the analysis with the Murava-Chernobyl (MC) fault zone. At its intersection with the KY fault, an alternation of high and low-resistivity objects can be observed in various depth intervals of the crust and upper mantle. A similar combination of high and low resistivity objects is also observed in the area of its intersection with the RN and YV faults. LROs along the MC fault can be assumed to be consistent with the NWGR at depths above 35 km. Metal minerals are associated with the Gusyatin – Volodarsk – Volyn (GVV) fault zone only northeast of the node of its intersection with the YV and OM faults. The chain of the low-resistivity features is confined to this area at depths reaching 20 km (with the conductance maximum at the depth of 9–12 km). The Khust – Korets (KK) fault intersects the studied area in its relatively short segment and its geoelectric parameters are therefore available only to a limited extent. High-resistivity features are located close to its intersection with the ULM fault zone and one of the graphite-bearing areas. The zone of intersection of the KK with the KY fault correlates with the ore node VI and is accompanied by local geoelectric heterogeneities at different depth intervals.

As follows from the above analysis, the majority of the identified conductive elements seems to be

controlled by fault zones and, like mineral concentrations, is tied with the fault junctions. The observed distribution of geoelectric parameters strongly depends both on the density of observation points and on the interpretation parameters. This conclusion is clearly visible when comparing the geoelectrical parameters obtained using 2D and 3D modelling (Fig. 6d, Fig. 7). Mineral locations displayed on maps refer to the upper crustal levels, and often the size of deposits and areas of high content of minerals with electron-type conductivity rarely exceed the first kilometers [Mineral…, I, 2006]. The largest are formations with high concentration of carbon material in the Early Proterozoic crystalline rocks. The average estimate of mineral concentration within the NWGR is 0.5–1 % [Yatsenko, 1998], the average graphite content within individual deposits is 4.6–6.7 % [Mineral…, II, 2006]. The extension of graphitized zones to depth is unclear. The erosional discordance varies from 13–18 km in the central part of the USh to about 30 km west of the longitude 30°E (Fig. 3b), indicating that graphitized rocks in neighbor areas are formed at depths differing by 10 km and more. Therefore, the graphitization recorded in the subsurface may continue at significant depths.

The different mechanisms of appearance of graphite in fault zones and its various forms (amorphous material as a result of friction in shear zones, transport and precipitation from fluids, destruction of carbonates) are outlined in [Cao and Neubauer, 2019]. The question of the carbon source origin itself is still debatable, which is largely determined by traditional ideas of the organogenic-syngenetic accumulation of carbonaceous matter and corresponding associations of ore elements. Nevertheless, innorganic origin of graphite is also permissible (e.g. [Van Zuilen et al., 2002; Glasby, 2006]), and according to another point of view, packs of high-carbon shales are considered as a result of superimposed graphitization (carbonization), with which the manifestations of U, Au, rare earth and other metals are spatially related. It should be noted that there are no fundamental objections to the hypothesis of a deep carbon source of the USh graphite deposits at present. For example, in [Yushin et al., 2013], the formation of complex, noble metal containing ore occurrences in carbon complexes is associated with the evolution of endogenous activity centers, which cau-sed the formation of ore associations. A similar relationship is assumed in [Mineral…, I, 2006].

Geoelectrics, like other geophysical methods, records the current state of the Earth, therefore, the observed electrical conductivity anomalies can be explained if we assume that the significant increase in conductivity of the rocks is due to the percolation effect. Percolation may be associated with the fluid flow in ancient weakened zones in the mantle. Along with model calculations of the influence of pore geometry and their permeability ([Shankland and Waff, 1977; Guion et al., 1989; Meng et al., 2019] and others) there are estimates of the percolation effect from field data. As follows from Fig. 9, both dependencies give a drop of by two orders of magnitude due to percolation phenomenon. It is difficult to assume that graphite is enriched in large volumes of rocks at depth without taking into account the connectivity of mineral inclusions. If we consider the presence of fluid degassing in certain places, then a significant decrease in such low resistivity objects seems to be acceptable.

The above analysis of conductive structures in the west of the USh suggests their link to active faults and their junctions, with a variety of ore mineralization zones, hydrocarbons and graphite that may have precipitated from fluids. Position of earthquake sources at the southwestern USh boundary, correlating with the increased heat flux, around the most conductive zones, again points to a relationship to neotectonic activity. The mechanisms governing activation processes on the USh are questionable. Although they can be attributed to the remote Alpine-Carpathian compressional deformations transmitted along the original fault systems [Starostenko et al., 2018], according to [Gordienko et al., 2020], current tectonic activity on the USh is not perceived as a kind of involvement in the activity of neighboring young structures and corresponds to the initial stages of rifting.

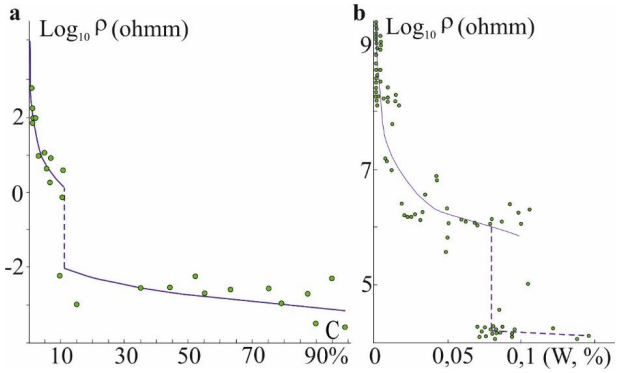

Fig. 9. The dependence of the electrical resistivity on: (a) the degree of water saturation (*W*) of typical crystalline rocks of the USh [Shepel, 2003]; (b) graphite content (*C*) in samples of graphite-containing minerals [Gordienko et al., 2005].

Originality

Areally imaged 2D and quasi-3D geoelectric models of the northwest of the USh are novel. They aim to elucidate the deep crustal and upper mantle structure and allow us to correlate the geoelectric features with fault systems and deposits of various natural mineral sources. Moreover, they can serve as possible evidence of tectonic activation processes in the studied area.

Practical significance

The presented results can bring social effect by identifying areas of mineral enrichment. In the field of geodynamics they can contribute to the assessment of natural hazard in mapping the course of tectonically active fault systems.

Conclusions

In addition to other phenomena, such as recent vertical movements of the earth's surface, increased heat flux and seismicity, the processes of tectonic activation of ancient terranes can manifest themselves by geoelectric anomalies originating in fluid transport along the re-activated fault systems. The presented analysis of geoelectric features of the western part of the Ukrainian Shield using electrical resistivity/ conductivity models allowed us to outline the connection of individual conductive features with faults active over the last 3 million years, their junctions and areas of mineralization with electron-type conductivity. Mineral deposits and their position relative to the faults indicate the nature of the appearance of accumulations of various elements associated with the fluid regime during activations. The obtained results allow (despite the insufficient density of the observation network and ambiguity in the interpretation of geoelectric data) their use to confirm the hypothesis of the relationship between ore and graphite deposits and zones of fluid generation and transportation (which determine the presence of conductive objects). They also contribute to the development of ideas about deep structure of the studied territory. Together with other geological and geophysical data, the presented information provides further evidence of current tectonic activity on the Shield. Further 3D inverse images will help to obtain a more complete picture of the deep structure of individual sections and better understand the geological architecture and geodynamic evolution of this region. However, in order to create a volumetric geoelectric model, it is desirable to expand the network of the MT observations to the eastern part of the territory which unfortunately falls within the Chernobyl accident zone.

Acknowledgement

The work was accomplished within the NASU project No 011U000117 “Deep processes in the crust and upper mantle of Ukraine and formation of ore mineral deposits”.

References

Antsiferov, A. V., Sheremet, E. M., Nikolaev, Yu. I., Nikolaev, I. Yu., Setaya, L. D., Antsiferov, V. A., & Omelchenko, A. A. (2011). Deep Electromagnetic (MT and AMT) Sounding of the Suture Zones of the Ukrainian Shield. *Izvestiya, Physics of the Solid Earth*, 47, 1, 33-44, https://doi.org/10.1134/ S106935 1311010010.

Astapenko, V. N. (2012). The Earth's crust and mantle on the territory of Belarus. Magnetotelluric data. Minsk. 208 p. (in Russian).

Astapenko, V. N., Logvinov, I. M. (2014). Geoelectric model of the crust and upper mantle along geotraverse EUROBRI-DGE-97. *Geofiz. Zhurn.*, 36, 5, 143-155 (in Russian). http://www.igph.kiev.ua/ FullVersion/2014/gj5/art5814.pdf

Banks, R. J. (1979). The use of the equivalent current systems in the interpretation of the Geomagnetic Deep Sounding data. *Geophys. J. R. Astr. Soc.*, 87, 139-157. https://doi.org/10.1111/j.1365-246X.1979. tb04773.x

Baysarovich, M. M., Mitropol'sky, O. Yu., ? Chuprina, I. C. (Eds.). (2002). Atlas. Deep lithospheric structure and eco-geology of Ukraine. Kiev: IGN NASU. 55 p. (in Ukrainian). https://doi.org 10.1016/j.gsf.2018. 10.011.

Bogdanova, S. R., Gorbatschev, R., Grad, M., Janik, T.A., Guterch, A., Kozlovskaya, E., Motuza, G., Skridlaite, G., Starostenko, V., Taran, L. (2006). EUROBRIDGE and POLONAISE Working Groups, 2006. EUROBRIDGE: new insight into the geo-dynamic evolution of the East European Craton. In: Gee, D.G., Stephenson, R.A. (eds). (2006). *European Lithosphere Dynamics*. Geological Society, London, Memoirs, 32, 599–625, https://doi.org/:10.1144/GSL.MEM.2006. 032.01. 36.

Bogdanova, S. V., Bingen, B., Gorbatschev, R., Kheraskova, T. N., Kozlov, V. I., Puchkov, V. N., Volozh, Yu. A. (2008). The East European Craton (Baltica) before and during the assembly of Rodinia. *Precam. Res.*, 160, 1, 23–45, doi:10. 1016/j.precamres.2007.04.024.

Bouzid, A., Bayou, B., Liégeois, J-P., Bourouis,S., Bougchiche, S.S., Bendekken, A., Abtout, A., Boukhlouf, W., Ouabadi, A. (2015), Lithospheric structure of the Atakor metacratonic volcanic swell (Hoggar, Tuareg Shield, southern Algeria): Electrical constraints from magnetotelluric data. *Geological Society of America Special Papers*, 71–514, 239–255, https://doi.org/:10.1130/2015. 2514(15).

Burakhovich, T. K., Kulik, S. N., Logvinov, I. M., Gordienko, I. V., & Tarasov, V. N. (1997). Conductivity crust of the NW Ukrainian Shield. *Reports of NAS of Ukraine*, 10, 125–128 (in Russian).

Cao, S., Neubauer, F. (2019). Graphitic material in fault zones: Implications for fault strength and carbon cycle. *Earth Sci. Rev.*, 194, 109–124, https://doi.org/10.1016/j.earscirev.2019.05.008.

Chattopadhyay, A., Bhattacharjee, D., Srivastava, S. (2020). Neotectonic fault movement and interpolate seismicity in the central Indian shield: a review and reappraisal. *Journal of Mineralogical and Petrological Sciences, J-STAGE Advance Publication*, 115, 2, 136–149. https://doi.org/10.2465/jmps.190824b.

Claesson, S., Bibikova, E., Shumlyanskyy, L., Dhuime, B., Hawkesworth, C.J. (2014). The oldest crust in the Ukrainian Shield – Eoarchaean U-Pb ages and Hf-Nd constraints from enderbites and metasediments. *Geological Society, London, Special Publications.* 389, 227–259. https://doi.org/10.1144/ SP389.9.

Foley, S. F. (2008). Rejuvenation and erosion of the cratonic lithosphere. *Nat. Geosci.*, 1, 503–510. https://doi.org/10.1038/ngeo261.

Garetsky, R. G., & Klushin, S. V. (1989). Listric faults in the Pripyat Trough. *Geotectonics*, 1, 48–60 (in Russian).

Gintov, O. B., Pashkevich, I. K. (2010). Tectonophysical analysis and geodynamic interpretation of the three-dimensional geophysical model of the Ukrainian Shield. *Geofiz. Zhurn*. 2, 32, 3-27 (in Russian).

Glasby, G. P. (2006). Abiogenic Origin of Hydrocarbons: A Historical Overview. *Resource Geology*, 56, 1, 83–96, https://doi.org/10.1111/j.1751–3928.2006.tb00271.

Gordienko, V. V., Gordienko, I. V., Zavgorodnyaya, O. V., & Usenko, O. V. (2002). Deep heat flow map of Ukraine. 1:2500000.

Gordienko, V. V., Gordienko, I. V., Zavgorodnyaya, O. V., Kovacikova, S., Logvinov, I. M., Tarasov, V. N., & Usenko, O. V. (2005). Ukrainian Shield (Geophysics, Deep Processes). Kiev: Korvin Press, 210 p. (in Russian). https://www.geokniga.org/bookfiles/geokniga-ukrainskiy-shchit.pdf

Gordienko, V.V., Gordienko, I.V., Zavgorodnyaya, O.V., Kovacikova, S., Logvinov, I.M., Pek, J.,Tarasov, V.N., Usenko, O.V. (2006). Dnepr-Donets Basin (Geophysics, Deep Processes). Kiev: Korvin Press, 210 p. (in Russian).

Gordienko, V. V., Gordienko, I. V., Zavgorodnyaya, O. V., Kovacikova, S., Logvinov, I. M., Tarasov, V. N., & Usenko, O. V. (2012). Volyn-Podolian Plate (Geophysics, Deep Processes). Naukova Dumka, Kiev. 180 p. (in Russian).

Gordienko, V. V., Gordienko, I. V., Gordienko, L. Ya., Zavgorodnyaya, O. V., Logvinov, I. M., & Tarasov, V. N. (2020). Zones of recent activation of Ukraine. *Geofiz. Zhurn.*, 2, 42, 29–52. https://doi.org/10.24028/gzh.0203-3100.v42i2.2020.201740.

Guion, E., Mitescu, K. D., Julien, J.P., Ru, S. (1989). Fractals and percolation in a porous medium. Fractals in Physics: Essays in Honour of Benoit B Mandelbrot. *Physics ser. D*. V. 38. 172–178.

Gursky, D. S., Kalinin, V. I., Gozhik, P. F., Velikanov, V. Ya., Kolosovskaya, V. A. (Eds.). (2003). Geology and minerals of Ukraine. Kiev: UkrGGRI. 368 p. (in Ukrainian).

Gursky, D. S., Kruglov, S. S. (Eds.). (2007). Tectonic map of Ukraine. 1:1000000. Kiev: UkrDGRI, 2007 (in Ukrainian).

Ilchenko, T. V. (2002). The results of research by the DSS transect EUROBRIDGE'97. *Geofiz. Zhurn*. 24, 3, 36–50 (In Russian).

Ingerov, A. I., Rokityansky, I. I., & Tregubenko, V. I. (1999). Forty years of MTS studies in Ukraine. *Earth Planet Space*, 51, 1127-1133.

Jodicke, H., Jording, A., Ferrari, L., Arzate, J., Mezger, K., & Rupke, L., 2006. Fluid release from the subducted Cocos plate and partial melting of the crust deduced from magnetotelluric studies in southern Mexico: Implications for the generation of volcanism and subduction dynamics. *J. Geophys. Res*. 111, B08102, https://doi.org/1029/2005JB003739.

Kaplun, V. B. (2018). Structure of the Zeya block of Toko Stanovik according to results of magnetotelluric soundings. *Russian Geology and Geophysics*, 59, 4, 419–431. https://doi.org/10.1016/j.rgg.2018.03.013.

Karato, S., & Wang, D. (2013). Electrical conductivity of minerals and rocks. In: Karato, S. (Ed.): Physicsand Chemistry of the Deep Earth. John Wiley & Sons, Ltd. https://doi.org/10.1002/9781 118529 492.ch5.

Kelbert, A., Meqbel, N., Egbert, G., & Tandon, K. (2014). ModEM: A modular system for inversion of electromagnetic geophysical data. *Computers & Geosciences*, 66, 40–53. https://doi.org/10.1016/ j.cageo. 2014.01.010.

Korja, T., Engels, M., Zhamaletdinov, A., Kovtun, A. A., Palshin, N. A., Smirnov, M. Yu., Tokarev, A. D., Asming, V. E., Vanyan, L. L., Vardaniants, I. L., & Bear W. G, 2002. Crustal conductivity in Fennoscandia – a compilation of a database on crustal conductance in the Fennoscandian Shield. *Earth Planets Space*, 54, 535–558.

Kováčiková S., Logvinov I., Nazarevych A., Nazarevych L., Pek J., Tarasov V., Kalenda P. (2016). Seismic activity and deep conductivity structure of the Eastern Carpathians. *Stud. Geophys. Geod.*, 60, 280–296. https://doi.org/10.1007/s11200-014-0942-y.

Kováčiková, S., Červ, V., Praus, O. (2005). Modelling of the conductance distribution at the eastern margin of the European Hercynides. *Studia geoph. et geod*., 49, 403–421.

Kováčiková, S., Logvinov, I., Tarasov, V. (2019). Comparison of the 2D and quasi-3D geoelectric models of the Ukrainian Eastern Carpathians and their link to the tectonic structure. *Tectonics*, 38, 3818–3834. https://doi.org/10.1029/2018TC0053 11.

Kovacikova, S., Logvinov, I. M., Pek J., & Tarasov V. N. (2016). Modelling of the Earth's crust of Ukraine by the results of the magnetotelluric studies using new methods of inversions. *Geofiz. Zhurn.*, 38, 6, 83–100. https://doi.org/10.24028/ gzh.0203-3100. v38i6.2016.91871.

Logvinov, I. M. (2015). Deep Geoelectrical Structure of the Central and Western Ukraine. *Acta Geophysica*, 63, 5, 1216–1230. https://doi.org/10. 1515/acgeo-2015-0049.

Logvinov, I. M., Gordienko, I. V., Tarasov, V. N. (2017). Geoelectric model (according to the 2D inversion of the results of magnetotelluric studies) along geotraverse DOBRE-3. *Reports of NAS of Ukraine*, 6, 148–165 (in Russian). https://doi.org/ 10.15407/dopovidi2018.04.067

Logvinov, I. M., & Tarasov, V. N. (2018). Electric resistivity distribution in the Earth's crust and upper mantle for the southern East European Platform and Crimea from area-wide 2D models. *Acta Geophys.*, 66, 2, 131–139. https://doi.org/10.1007/ s11600-018-0125-2.

Logvinov, I. M., Tarasov, V. N. (2019). Electric resistivity distribution in the Earth's crust and upper mantle for the western East European Platform in Ukraine from area-wide 2D models. *Geofiz. Zhurn.*, 41**,** 1, 44–75 (in Russian), https://doi.org/ 1024028/ gzh0203-3001.v.41i1.2019.158863.

Logvinov, I. M., Tarasov, V. N., Gordienko, I. V. (2020). Geoelectric parameters of the northwestern Ukrainian Shield from 2D inversion. *Geofiz. Zhurn.*, 42, 1, 51–64 (in Russian). https://doi.org/10.24028/ gzh.0203-3100.v42i1.2020.195467.

Lough, A. C., Wiens, D. A., Nyblade, A. (2018). Reactivation of ancient Antarctic rift zones by intraplate seismicity. *Nature Geoscience*, 11, 515–519. https://doi.org/10.1038/s4156 1-018-0140-6.

Makhnach, A. S., Garetsky, R. G., Matveev, A. V. (Eds.) (2001). Geology of Belarus. Minsk: Institute of Geological Sciences of the National Academy of Sciences of Belarus. 815 pp. (in Russian).

Malleswari, D., Veeraswamy, K., Abdul-Azeez, K.K., Gupta, A. K., Babu, N., Patro, P. K., & Harinarayana, T. (2019). Magnetotelluric incvestigation of lithosphe-ric electrical structure beneath the Dharwar Craton in South India: Evidence for mantle suture and plume-continental interaction. *Geosci. Front.*, 10, 1915–1930. https://doi.org/ 10.1016/j.gsf. 2018.10.011.

Map of the hypsometry of the sole of the plate complexes of the southwest of the USSR (using space survey materials). 1: 1000000. (1988). Ed. N.A. Krylov. Moscow: Mingeo USSR, 41 (in Russian).

Map of the location of oil and gas prospective provinces and areas of Ukraine by geophysical data. 1:4000000 (2004). Ed. V. I. Starostenko. Kyiv: Ukr.DGRI (in Ukrainian).

Meng, H., Shi, Q., Liu, T., Liu, F.X, & Chen, P. (2019). The percolation properties of electrical conductivity and permeability for fractal porous media. Energies, 12.1085. https://doi.org/ 10.33990/en12 061085.

Shcherbak, M. P., & Bobrov, O. B. (2006). Mineral deposits of Ukraine. I: Metalliferous mineral deposits. Kyiv – Lviv. "Centre of Europe" Publ. House, 785 p. (in Ukrainian).

Parfeevets, A.V., Sankov, V.A., 2018. Geodynamic Conditions for Cenozoic Activation of Tectonic Structures in Southeastern Mongolia. *Geodynamics and Tectonophysics*, Publ. of the Earth's Crust Siberian Branch, RAS, 9, 3, 855–888. https://doi.org/10.5800/GT-2018-9-3-0374.

Prikhodko, V. L., & Prikhodko, M. V. (2005). Trapezoidal formation of Volyn and native-mineral fertilization. *Collection of scientific works of UkrDGRI*, 1, 101–109 (in Ukrainian).

Ryabenko, V. A. (1970). The main features of the tectonic structure of the Ukrainian crystalline shield. Kyiv: Nauk. Dumka, 128 p. (in Russian).

Salishchev, K. A. (1987). Design and mapping. Moscow. MSU Publishing House, 240 p. (in Russian).

Sarafian, E., Evans, R. L., Abdelsalam, M. G., Atekwana, E., Elsenbeck, J., Jones, A. G., & Chikambwe, E. (2018). Crustal conductors along shear and suture zones – graphite and sulphides that experienced shearand metamorphism. *Gondwana Res.*, 54, 38–49. https://doi.org/ 10.1016/j.gr.2017.09. 007.

Semenov, V. Y., Pek, J., Adam, A., Jozwiak, W., Ladanyvskyy, B., Logvinov, I., Pushkarev, P., & Vozar J. (2008). Electrical structure of the upper mantle beneath Central Europe: Results of the CEMES project. *Acta Geophysica*, 56, 4, 957–981. https://doi.org/10.2478/s11600-008-0058-2.

Shankland, T., Waff, H. (1977). Partial melting and electrical conductivity anomalies in the Upper Mantle. *J. Geophys. Res.*, 82, 33, 5409–5417.

Shepel, S. I. (2003). Electrical properties of rocks under thermobaric conditions of the lithosphere and geoelectric models. Habil. Thesis 04.00.22, Kiev, 2003, 411 p. (in Russian).

Shirkov B. I., Burakhovich, T. K., & Kushnir, A. N. (2017). Three-dimensional geoelectric model of the Golovanevsk suture zone of the Ukrainian Shield. *Geofiz. Zhurn.*, 1, 39, 41–60 (in Russian), https://doi.org/10.24028/gzh.0203-3100.v39i1. 2017.94010.

Siripunvaraporn, W., Egbert, G. (2000). An efficient data-subspace inversion method for 2-D magnetotelluric data. *Geophysics*, 65, 3, 791–803.

Siripunvaraporn, W., Egbert, G., Lenbury, Y., Uyeshima, M. (2005). Three-dimensional magnetotelluric inversion: data-space method. *Phys. Earth Planet. Interiors*. 150, 3–14, https://doi.org/10.1016/j.pepi. 2004.08.023.

Sollogub, V. B., 1980. Lithosphere of Ukraine. Kiev: Nauk. Dumka, 184 p. (in Russian).

Srebrov, B., Logvinov, I., Rakhlin, L., Kováčiková, S. (2018). Results of the magnetotelluric investigations at geophysical observatories in Bulgaria. *Geophys. J. Int*., 215, 165–180, https://doi.org/10.1093/gji/ ggy268.

Starostenko, V., Janik, T., Yegorova, T., Czuba, W., Sroda, P., Lysynchuk, D., Aizberg, R., Garetsky, R., Karataev, G., Gribik, Y., Farfuliak, L., Kolomiyets, K., Omelchenko, V., Komminaho, K., Tiira, T., Gryn, D., Guterch, A., Legostaeva, O., Thybo, H., & Tolkunov, A. (2018). Lithospheric structure along wide-angle seismic profile GEORIFT 2013 in Pripyat – Dnieper – Donets Basin (Belarus and Ukraine). *Geophys. J. Int*., 212,1932–1962, https://doi.org/10.1093/gji/ggx 509.

Tarasov, V. N., & Logvinov, I. M. (2020). Using the TAR3D program for 3D data visualization in geoelectric studies. Proceedings of the conference *Geoinformatics, Theoretical and Applied Aspects*, 2020, 1–5, https://doi.org/10.3997/2214-4609. 2020geo020.

Thybo, H., Janik, T., Omelchenko, V. D., Grad, M., Garetsky, R. G., Belinsky, A.A., Karatayev, G. I., Zlotski, G., Knudsen, E., Sand, R., Yliniemi, J., Tiiro, T., Luosto, U., Komminaho, K., Giese, R., Guterch, A., Lund, C.E., Kharitonov, O.M., Ilchenko, T. V., Lysynchuk, D. V., Skobolev, V. M., & Doody, J. J. (2003). Upper lithospheric seismic velocity structure across the Pripyat Trough and the Ukrainian Shield along the EUROBRIDGE'97 profile. *Tectonophysics* 371, 1/4, 41–79, https://doi.org/10.1016/S0040-1951(03)00200-2.

Tregubenko, V. I., Lukin, O. E., Kremnetsky, O. O., Petrovsky, O. P., Kostenko, M. M., Slonitska, S. G, Shimkiv, L. M., Nikitash, O. B, Dzyuba, B. M., Nechaeva, T. S, & Ipatenko, S. P. (2009). Investigation of anomalous geophysical zones of the Ukrainian Shield adjacent to oil-gas basins with the method of evaluation of their oil and gas content (2005–2009). Kyiv: Geoinform. 405 p. (in Ukrainian).

Unsworth, M., & Bedrosian, P. A. (2004). On the geoelectric structure of major strike-slip faults and hear zones. *Earth Planet Space*, 56, 12, 1177-1184. https://earth-planets-space.springeropen.com/articles/10.1186/BF03353337.

Usenko, I. S. (Ed.) (1982). Metamorpism of the Ukrainian shield. Kiev: Naukova Dumka. 1982. 307 p. (in Russian).

Van Zuilen, M. A., Lepland, A., & Arrhenius, G. (2002). Reassessing the evidence for the earliest traces of life. *Letters to Nature*, 418, 627–630, https: //www.nature.com/articles/nature00934.

Verkhovtsev, V. (2006). Newest vertical crustal movements in Ukraine, their relationship with linear and circular structures. *In: Power Earth, its geological and environmental displays, scientific and practical use.* Kyiv: KNU. 129–137 (in Ukrainian).

Wang, H., van Hunen, J., & Pearson, D. G. (2015). The thinning of subcontinental lithosphere: The roles of plume impact and metasomatic weakening. *Geochem. Geophys. Geosyst*., 16, 1156–1171, https://doi.org/10.1002/2015GC005748.

Wu, P., Johnston, P., & Lambeck, K. (1999). Postglacial rebound and fault instability in Fennoscandia. *Geophys. J. Int*., 139, 657–670.

Yatsenko, V. G. (1998). Regularities of the spatial arrangement of graphite manifestations on the Ukrainian shield. *Aspects of mineralogy in Ukraine*. Kiyv: GNC ROS. 254-270 (in Russian).

Yin, Y., Unsworth, M., Liddell, M., Pana, D., & Craven, J.A. (2014). Electrical resistivity structure of the Great Slave Lake shear zone, northwest Canada: implications for tectonic history. *Geophys. J. Int*., 199, 178-199, doi:10.1093/gji/ggu251.

Yushyn, A. A., Moroz, V. S., & Proskurko, L. I. (2013). Genetic peculiarities of manifestations of precious and non-ferrous metals mineralization in carboniferous complexes of the Early Pre-Cambrian at the Krivoi Rih basin. *Geology and Mineralogy Bulletin of the Krivoi Rih National University*, 1–2, 12–18, (in Russian).

Світлана КОВАЧІКОВА[1], Ігор ЛОГВІНОВ[2'], Віктор ТАРАСОВ[2]

[1] Інститут геофізики, АН Чеської республіки, Бочні II/1401, Прага 4-14131, Чеська республіка, ел. пошта: svk@ig.cas.cz, https://doi.org/0000-0003-2600-175X
[2] Інститут геофізики ім. С. І. Субботіна Національної академії наук України, пр. Академіка Палладіна, Київ, 03142, Україна, ел. пошта: anna_log@ukr.net, https://doi.org/0000-0002-9584-0314

2D ТА КВАЗІ-3D ГЕОЕЛЕКТРИЧНІ МОДЕЛІ ЗЕМНОЇ КОРИ ТА ВЕРХНЬОЇ МАНТІЇ ЯК МОЖЛИВЕ СВІДЧЕННЯ НЕДАВНЬОЇ ТЕКТОНІЧНОЇ АКТИВНОСТІ В ЗАХІДНІЙ ЧАСТИНІ УКРАЇНСЬКОГО ЩИТА

Мета роботи – моделювання розподілу електропровідності в північно-західній частині Українського щита та вивчення взаємозв'язку геоелектричних аномалій із природними родовищами корисних копалин та з ознаками можливої тектонічної активізації довгоіснуючих систем розломів на щиті. Методологія досліджень основана на довгоперіодних магнітотеллурічних і магнітоваріаційних вимірюваннях в діапазоні періодів від 3–16 до 2500–3600 с. Густа мережа пунктів вимірювань дала змогу дослідити геоелектричну структуру сегмента Українського щита, обмеженого координатами 26°–30°E та 48°–51,7°N. 2D та квазі-3D інверсії отриманих магнітотеллуричних та геомагнітних відгуків привели до створення оглядових моделей питомого електроопору/провідності для території досліджень. В результаті на різних глибинах були виявлені геоелектрично аномальні структури. Локальний характер провідників та їхнє положення вказують на їх зв'язок із нещодавно активованими зонами розломів, місцями їх перетину та з металогенезом. Докембрійський вік кристалічних порід досліджуваної території вказує на переважно електронний тип графітно-сульфітного походження підвищеної електропровідності, однак глибина провідних аномалій, їх вертикальна протяжність і зв'язок з оновленими системами розломів можуть свідчити про генетичний зв'язок різних мінералів і їх подальше осадження з глибинною міграцією флюїдів. **Наукова новизна.** Отримані результати спрямовані на з'ясування глибинної будови та співвіднесення геоелектричних особливостей земної кори та верхньої мантії з системами розломів та родовищ різних корисних копалин і самі по собі можуть бути додатковим свідченням можливих тектонічних активізаційних процесів на досліджуваній території. **Практична значущість.** Подані результати можуть принести економічну користь завдяки визначенню районів наявності мінеральної сировини, а у вивченні геодинаміки можуть сприяти оцінюванню природної небезпеки під час картографування простягання тектонічно активних систем розломів.

Ключові слова: земна кора і верхня мантія; Східноєвропейська платформа; Український щит; електропровідність; мінералізація.

Received 15.05.2020